Inorganic Chemistry

Article

pubs.acs.org/IC

Tetra-2,3-pyrazinoporphyrazines with Externally Appended Pyridine Rings. 12. New Heteropentanuclear Complexes Carrying Four Exocyclic Cis-platin-like Functionalities as Potential Bimodal (PDT/Cis-platin) Anticancer Agents

Maria Pia Donzello,*[,†] Elisa Viola,[†] Claudio Ercolani,[†] Zhen Fu,[‡] David Futur,[‡] and Karl M. Kadish*[,‡]

[†]Dipartimento di Chimica, Università degli Studi di Roma "La Sapienza", P.le A. Moro 5, I-00185 Roma, Italy

[‡]Department of Chemistry, University of Houston, Houston, Texas, 77204-5003, United States

Supporting Information

ABSTRACT: Heteropentanuclear porphyrazines having the formula $[(PtCl_2)_4LM]$ where L = tetrakis-2,3-[5,6-di(2-pyridyl)-pyrazino]porphyrazinato dianion and M = Zn^{II}, $Mg^{II}(H_2O)$, Pd^{II}, Cu^{II} or Co^{II} were characterized by elemental analyses, IR−UV−visible spectroscopy and electrochemistry and the data compared to new and previously published results for the corresponding homopentanuclear compound $[(PtCl_2)_4LPt]$. This latter species has four external $N_{2(py)}PtCl_2$ coordination sites which closely resemble cis-platin, $(NH_3)_2PtCl_2$, the potent chemotherapeutic anticancer drug, and is able to act as a photosensitizer for the generation of $^1O_2$, the cytotoxic agent in photodynamic therapy (PDT). UV−visible spectra and half wave potentials for reduction of $[(PtCl_2)_4LM]$, $[(PtCl_2)_4LPt]$, the parallel series of mononuclear [LM] compounds and the pentanuclear $[(PdCl_2)_4LM]$ compounds were examined in the nonaqueous solvents dimethyl sulfoxide, pyridine, and dimethylformamide. The complete set of available data indicate that external coordination of the $PtCl_2$ and $PdCl_2$ units significantly increases the level of the electron-deficiency of the entire molecular framework despite the fact that these groups are far away from the central porphyrazine π-ring system and have coordination sites nearly orthogonal to the plane of the macrocycle. The pentanuclear species $[(M'Cl_2)_4LM]$ (M′ = Pt^{II}, Pd^{II}) undergo multiple one-electron transfers and exhibit an easier reducibility as compared to related electrode reactions of the parent compounds [LM] having the same central metal. Aggregation phenomena and reducibility of the porphyrazines to their monoanionic form (prevalently in DMF) are observed for some of the examined compounds and were analyzed and accurately taken into account. Quantum yields of $^1O_2$ (Φ_Δ), of interest in PDT, were measured for $[(PtCl_2)_4LM]$ with M = Zn^{II}, $Mg^{II}(H_2O)$, or Pd^{II} and the related macrocycles $[(PdCl_2)_4LM]$ and [LM] in dimethylformamide (DMF) and/or DMF preacidified with HCl (DMF/HCl, [HCl]: $1-2 \times 10^{-4}$ M). Excellent Φ_Δ values (0.5−0.6) which qualify the compounds as potent photosensitizers in PDT were obtained for the pentanuclear species having Zn^{II} or Pd^{II} as central metal ions. The $[(PtCl_2)_4LZn]$ and $[(PtCl_2)_4LPd]$ complexes are of special interest as potential bimodal anticancer agents because of the incorporated four cis-platin-like functionalities.

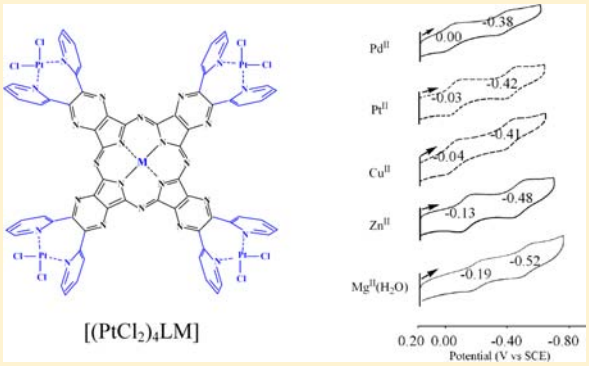

INTRODUCTION

Porphyrins are active photosensitizers, able to absorb light in the visible region and generate singlet oxygen, $^1O_2$, the main cytotoxic agent in photodynamic therapy (PDT), a nowadays widely used anticancer curative modality.[1] Porphyrins, however, exhibit weak absorptions in the phototherapeutic spectral window (600−850 nm), this requiring high dosages in PDT; in addition, they induce long-lasting skin photosensitivity. Unlike the porphyrins, phthalocyanines, typical porphyrin-like macrocycles, and porphyrazines in general, normally show intense absorption bands in the therapeutic window. Thus, phthalocyanines[1d,e,2] and various types of porphyrazine macrocycles, that is, tetrapyrazinoporphyrazines,[3] secoporphyrazines,[4] and benzonaphthoporphyrazines[5] have been actively considered as promising photosensitizers in PDT.

An exploration of the combined action of PDT with chemo- or radiotherapies is currently of great interest as a curative therapy against cancer. For many years (and still today), the most widely used chemotherapeutic drug for treating a variety of tumors has been cis-platin, $(NH_3)_2PtCl_2$, with only a few other analogues (carboplatin, oxaliplatin) apparently able to approach the efficacy of the basic material.[6] Because cis-platin is highly toxic for nontumor cells, its use in association with PDT might lead to a more moderate use of this drug. Along these lines, cis-platin and porphyrin photosensitizers have been used together as two distinct molecular systems.[7] A cis-platin-like function has also been inserted peripherally into porphyrins and

Received: September 12, 2012
Published: November 2, 2012

   dx.doi.org/10.1021/ic301989a | *Inorg. Chem.* 2012, 51, 12548−12559

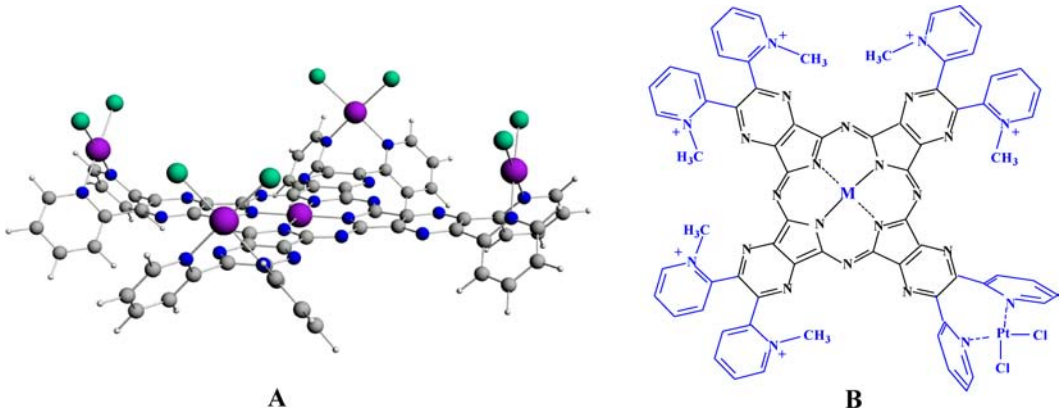

Figure 1. Schematic representation of (A) the widely prevalent structural component of $[(PdCl_2)_4LPd]$ bearing all four external $N_{2(py)}PdCl_2$ moieties oriented on the same side of the central pyrazinoporphyrazine core (4:0 arrangement);[11] (B) the heterobimetallic hexacations $[(PtCl_2)(CH_3)_6LM]^{6+}$ (M = Zn^{II}, $Mg^{II}(H_2O)$, Pd^{II}).[13]

related macrocycles,[8] but because of the low solubility of phthalocyanines and porphyrazines in water, there have been only a few reports on the anticancer activity of these systems when tested as a separate entity with cis-platin[9] or when joined together in the same molecular framework.[10]

In our own studies of PDT, it was found that a triad of Pd^{II} macrocycles, formulated as [LPd], $[(PdCl_2)_4LPd]$ (Figure 1A) and $[(CH_3)_8LPd]^{8+}$ (neutralized by I^- ions) where L = tetrakis-2,3-[5,6-di(2-pyridiyl)pyrazino]porphyrazine, behave as excellent photosensitizers for the production of $^1O_2$.[11−14] A related Zn^{II} complex, $[(CH_3)_8LZn]^{8+}$ also shows high photoactivity in PDT.[13] Interestingly, this Zn^{II} octacation is able to bind to the single stranded telomeric DNA guanine-rich sequence 5′-d[AGGG(TTAGGG)$_3$]-3′ which is present as a G-quadruplex-type structure (G4) in aqueous solutions containing K^+ or Na^+ ions.[15]The binding to G4 drives the conformational equilibrium of the telomeric sequence exclusively toward a "parallel" conformation. This observation indicates that this octacation is a potential agent for bimodal anticancer therapy. A similar combined PDT/G4 study was performed on the hexacationic complex $[(PtCl_2)(CH_3)_6LZn]^{6+}$, selected from the series of heterobimetallic species of the form $[(PtCl_2)(CH_3)_6LM]^{6+}$ (M = $Mg^{II}(H_2O)$, Zn^{II}, Pd^{II}) (Figure 1B).[13] The Zn^{II}/Pt^{II} complex was proved to possess PDT/G4 bimodal anticancer potentialities.[16] A potential multimodal anticancer applicability, presently under examination, is open for this compound because of the presence of a cis-platin-like functionality at the macrocycle periphery.

The synthesis and physicochemical characterization of three Pt^{II} complexes which parallel the triad of Pd^{II} analogues mentioned above, [LPt], $[(PtCl_2)_4LPt]$, and $[(CH_3)_8LPt](I)_8$, have also been reported.[14] Among them, $[(PtCl_2)_4LPt]$, based on NMR spectral data, was shown to have a structure similar to that of the Pd^{II} analogue, $[(PdCl_2)_4LPd]$ (Figure 1A; 4:0 isomer) and this was also the case for other compounds in the series of $[(PdCl_2)_4LM]$ where M = Zn^{II}, $Mg^{II}(H_2O)$, Cu^{II} and Cd^{II}.[17] Interestingly, these findings appear to suggest that the 4:0 arrangement shown in Figure 1A for $[(PdCl_2)_4LPd]$ is largely predominant in all the $[(M'Cl_2)_4LM]$ species, independent of either the type of external $M'Cl_2$ unit (M′ = Pd^{II}, Pt^{II}) or the central metal ion for derivatives with M = $Mg^{II}(H_2O)$, Zn^{II}, Pd^{II}, Pt^{II}, Cu^{II} or Cd^{II}.

$[(PtCl_2)_4LPt]$, which is moderately photoactive for the generation of $^1O_2$ (quantum yield value Φ_Δ = 0.36)[14] and hence of interest in PDT, shows bimodal anticancer potentialities in that it possesses the rare feature of having four cis-platin-like functionalities in the structure. In the light of this fact and the above considerations, it was believed of interest to extend our measurements of Φ_Δ to a series of new related pentanuclear heterometallic compounds represented as $[(PtCl_2)_4LM]$ where M = $Mg^{II}(H_2O)$, Zn^{II}, or Pd^{II}. These new porphyrazines were also investigated as to their spectroscopic and electrochemical behavior, in addition to being examined as to their photosensitizing activity. A characterization of the Cu^{II} and Co^{II} analogues is also included in the present study, although electrochemistry of the Co^{II} compound containing $PtCl_2$ units could not be obtained because of extensive aggregation under all solution conditions. A comparison of the photosensitizing properties of the $[(PtCl_2)_4LM]$ compounds is made with that of the $[(PdCl_2)_4LM]$ analogues (M = $Mg^{II}(H_2O)$, Zn^{II}, Pd^{II}), whose quantum yields of $^1O_2$ (Φ_Δ) were not previously examined.[17]

EXPERIMENTAL SECTION

Solvents and Reagents. All chemical reagents were commercially purchased and used as received, including 1,3-diphenylisobenzofuran (DPBF, 97% Aldrich) and chlorophyll-a (Sigma-Aldrich, free of chlorophyll-b), which was kept in the refrigerator at −20 °C. Dimethyl sulfoxide (DMSO) was freshly distilled over CaH_2 before use. Other solvents, including dimethylformamide (DMF, C. Erba RPE), were used as received. The mononuclear complexes [LM] (M = $Mg^{II}(H_2O)$, Zn^{II}, Cu^{II}, Co^{II})[18] and the corresponding Pd^{II} species[11] were obtained as previously reported. Experimental details for preparation of the newly synthesized $[(PtCl_2)_4LM]$ (M = $Mg^{II}(H_2O)$, Zn^{II}, Pd^{II}, Cu^{II}, Co^{II}) and $[(PdCl_2)_4LCo]$ are given here below.

Synthesis of $[(PtCl_2)_4LMg(H_2O)]\cdot 12H_2O$. $[LMg(H_2O)]\cdot 4H_2O$ (30.5 mg, 0.024 mmol) was suspended (partly dissolved) in freshly distilled DMSO (1.5 mL), $PtCl_2$ (59.6 mg, 0.224 mmol) added, and the mixture heated at 120 °C for 22 h. After cooling, the solid material was separated by centrifugation, washed with water and acetone, and brought to constant weight under vacuum (10^{-2} mmHg) (39.4 mg, yield 67%). Calcd for $[(PtCl_2)_4LMg(H_2O)]\cdot 12H_2O$, $C_{64}H_{58}Cl_8MgN_{24}O_{13}Pt_4$: C, 31.25; H, 2.38; N, 13.67; Pt, 31.73. Found C, 30.72; H, 2.24; N, 12.43; Pt, 32.27%. IR (cm^{-1}, KBr): 3425 m (broad), 1682 w, 1624 w, 1603 m, 1557 w-m, 1485 s, 1437 w, 1418 vvw, 1360 s, 1290 w, 1244 vs, 1190 m-s, 1163 m, 1123 m, 1107 m, 1090 m, 1069 vvw, 1038 w, 972 vvw, 955 m-s, 893 w, 860 w, 822 w, 775 s, 710 vs, 690 w, 656 w-m, 619 vvw, 582 vvw, 559 w-m, 528 vvw, 509 vvw, 494 vw, 463 vvw, 438 w-m, 350 m (ν_{Pt-Cl}). It should be noted that the Mg^{II} complex, $[(PtCl_2)_4LMg(H_2O)]$, like its analogue carrying externally $PdCl_2$ units, $[(PdCl_2)_4LMg(H_2O)]$,[17] may undergo

dx.doi.org/10.1021/ic301989a | Inorg. Chem. 2012, 51, 12548−12559

a transmetalation process, $Mg^{II}(H_2O) \rightarrow Pt^{II}$ during the synthetic procedure, leading to materials containing the pentaplatinated species $[(PtCl_2)_4LPt]$ as a contaminant, the amount of which varied from minimal to significant, depending on the batch preparation (see further discussion below on this point). The synthetic procedure reported above refers to one in which a negligible amount of "contaminant" was formed.

Synthesis of $[(PtCl_2)_4LZn]\cdot 15H_2O$. $[LZn]\cdot 5H_2O$ (31.1 mg, 0.024 mmol) was suspended (partly dissolved) in freshly distilled DMSO (1.5 mL), $PtCl_2$ (49.5 mg, 0.186 mmol) added, and the mixture heated at 120 °C for 22 h. After cooling, the solid material was separated by centrifugation, washed with water and acetone, and then brought to constant weight under vacuum (10^{-2} mmHg) (42.2 mg, yield 69%). Calcd for $[(PtCl_2)_4LZn]\cdot 15H_2O$, $C_{64}H_{62}Cl_8N_{24}O_{15}Pt_4Zn$: C, 30.30; H, 2.46; N, 13.25; Pt, 30.76. Found C, 30.74; H, 2.14; N, 12.09; Pt, 30.80%. IR (cm^{-1}, KBr): 3500 m (broad), 1624 w, 1603 m, 1553 m, 1487 s, 1437 w, 1416 w, 1362 s, 1290 w, 1244 vs, 1196 m-s, 1163 vw, 1123 m-s, 1107 m-s, 1096 m, 1067 vvw, 1038 w, 957 s, 893 w, 856 w, 822 w, 789 w, 772 s, 744 w, 708 vs, 690 w, 656 m, 617 w, 582 vw, 559 w-m, 507 w, 494 w, 461 vvw, 436 w-m, 350 m (ν_{Pt-Cl}).

Synthesis of $[(PtCl_2)_4LPd]\cdot 10H_2O$. $[LPd]\cdot 10H_2O$ (32.6 mg, 0.023 mmol) was suspended (partly dissolved) in freshly distilled DMSO (1.5 mL), $PtCl_2$ (54.8 mg, 0.206 mmol) added, and the mixture heated at 120 °C for 22 h. After cooling, the solid material was separated by centrifugation, washed with water and acetone, and brought to constant weight under vacuum (10^{-2} mmHg) (39.2 mg, yield 69%). Calcd for $[(PtCl_2)_4LPd]\cdot 10H_2O$, $C_{64}H_{52}Cl_8N_{24}O_{10}PdPt_4$: C, 30.90; H, 2.11; N, 13.51; Pd, 4.28; Pt, 31.37. Found C, 31.48; H, 2.31; N, 12.03; Pd, 5.64; Pt, 29.93%. IR (cm^{-1}, KBr): 3500 w-m (broad), 1624 w, 1601 m, 1558 m, 1518 w-m, 1485 m, 1437 w, 1356 s, 1292 vw, 1248 vs, 1192 m-s, 1163 vw, 1132 s, 1092 vw, 1065 vw, 1038 w, 970 m-s, 881 w, 812 w-m, 773 m-s, 754 w, 714 vs, 689 vw, 658 w-m, 619 vvw, 579 vvw, 559 w-m, 507 w, 461 vvw, 442 w-m, 420 vvw, 350 m (ν_{Pt-Cl}).

Synthesis of $[(PtCl_2)_4LCu]\cdot 20H_2O$. $[LCu]\cdot 7H_2O$ (32.5 mg, 0.024 mmol) was suspended in freshly distilled DMSO (1.5 mL), $PtCl_2$ (51.9 mg, 0.195 mmol) was added, and the mixture heated at 120 °C for 22 h. After cooling and addition of acetone (6 mL) the suspension was kept overnight in the refrigerator. After centrifugation, the solid was separated from the mother liquor, washed with water and acetone, and brought to constant weight under vacuum (10^{-2} mmHg) (24.8 mg, yield 39%). Calcd for $[(PtCl_2)_4LCu]\cdot 20H_2O$, $C_{64}H_{72}Cl_8CuN_{24}O_{20}Pt_4$: C, 29.28; H, 2.76; N, 12.81; Pt, 29.73. Found C, 28.81; H, 2.78; N, 12.16; Pt, 29.10%. IR (cm^{-1}, KBr): 3520 w-m (broad), 1632 vw, 1600 m, 1556 m-s, 1538 w-m, 1485 m, 1433 w, 1413 w, 1360 s, 1294 w, 1245 vs, 1196 m, 1163 vw, 1124 s, 1093 w, 1020 m-s, 962 m-s, 885 vvw, 867 vw, 823 vw, 805 vw, 769 m-s, 754 m-s, 710 vs, 657 w-m, 560 m, 508 vw, 461 vw, 438 m, 380 w, 340 m-s (ν_{Pt-Cl}).

Synthesis of $[(PtCl_2)_4LCo]\cdot 8H_2O$. $[LCo]\cdot 4H_2O$ (68.4 mg, 0.054 mmol) was suspended in freshly distilled DMSO (1.5 mL), $PtCl_2$ (109.6 mg, 0.412 mmol) was added, and the mixture heated at 120 °C for 22 h. After cooling, the solid material was separated by centrifugation, washed with water and acetone, and brought to constant weight under vacuum (10^{-2} mmHg) (122.5 mg, yield 94%). Calcd for $[(PtCl_2)_4LCo]\cdot 8H_2O$, $C_{64}H_{48}Cl_8CoN_{24}O_8Pt_4$: C, 31.97; H, 2.01; N, 13.98; Pt, 32.46. Found C, 32.08; H, 1.98; N, 12.33; Pt, 33.20%. IR (cm^{-1}, KBr): 3580 w-m (broad), 3077 w, 1601 w-m, 1562 s, 1527 m, 1483 m, 1435 w, 1360 s, 1344 s, 1294 vw, 1246 vs, 1193 m-s, 1131 s, 1064 w, 1037 vw, 971 m, 949 w, 820 vw, 806 w, 771 m-s, 757 s, 712 vs, 658 w, 561 w, 508 w, 441 w-m, 344 m/336 m (ν_{Pt-Cl}).

Synthesis of $[(PdCl_2)_4LCo]\cdot 9H_2O$. $[LCo]\cdot 4H_2O$ (80.5 mg, 0.063 mmol) was suspended in freshly distilled DMSO (1.5 mL), $PtCl_2$ (67.1 mg, 0.378 mmol) was added, and the mixture heated at 120 °C for 5 h. After cooling, the solid material was separated by centrifugation, washed with water and acetone, and brought to constant weight under vacuum (10^{-2} mmHg) (121.7 mg, yield 93%). Calcd for $[(PdCl_2)_4LCo]\cdot 9H_2O$, $C_{64}H_{50}Cl_8CoN_{24}O_9Pd_4$: C, 37.18; H, 2.44; N, 16.26; Pd, 20.59. Found C, 37.20; H, 2.61; N, 14.55; Pd, 19.35%. IR (cm^{-1}, KBr): 3580 w-m (broad), 3072 w, 1598 w-m, 1561 m-s, 1525 w-m, 1483 m, 1433 vvw, 1358 m-s, 1343 s, 1293 vw, 1247 vs, 1186 m, 1163 w, 1131 s, 1059 vw, 1033 w, 971 m, 822 w, 806 w, 774 m, 755 s, 713 vs, 660 w, 560 w-m, 507 vw, 442 w-m, 347 w/334 vw (ν_{Pd-Cl}).

Electrochemical and Spectroelectrochemical Measurements. Cyclic voltammetry was performed with an EG&G Model 173 Potentiostat coupled to an EG&G Model 175 Universal Programmer. Current–voltage curves were recorded on an EG&G Princeton Applied Research model R-0151 X-Y recorder. A three-electrode system was used, consisting of a glassy carbon working electrode, a platinum counter electrode and a saturated calomel reference electrode (SCE). UV–visible spectroelectrochemical experiments were carried out with a homemade thin-layer cell which has a light-transparent platinum gauze working electrode.[19] The applied potential was monitored with an EG&G Model 173 potentiostat, and UV–visible spectra were recorded on a Hewlett-Packard Model 8453 diode array spectrophotometer.

The solvents used for electrochemical measurements, pyridine (99.9+%), dimethyl sulfoxide (DMSO, 99.9+%), and *N*,*N*-dimethylformamide (DMF, 99.8+%), were purchased from Sigma-Aldrich Co. and used without further purification. High purity N_2 from Trigas was used to deoxygenate the solution before each electrochemical and spectroelectrochemical experiment. Tetra-*n*-butylammonium perchlorate (TBAP, 99%) from Fluka Chemika Co. was used as supporting electrolyte (0.1 M for cyclic voltammetry and 0.2 M for spectroelectrochemistry) and stored under vacuum at 40 °C prior to use.

Singlet Oxygen Quantum Yields Measurements. Singlet oxygen quantum yields (Φ_Δ) of the complexes were determined in DMF with and without added aqueous HCl (DMF/HCl, [HCl] = (1–2) × 10^{-4} M; $\%V_{H2O}$ = (0.05–0.1)%) by an absolute method employing 1,3-diphenylisobenzofuran (DPBF) as chemical quencher for singlet oxygen. An experimental procedure previously reported in the literature[2b,5] was modified as described in a recent publication.[20] Details are as follows: solutions of the complex (ca. 10^{-6}–10^{-5} M) and DPBF (ca. 5 × 10^{-5} M) in DMF or in DMF/HCl were irradiated with appropriate laser light (Premier LC Lasers/HG Lens, Global Laser) at a wavelength, λ_{irr}, close to the Q-band absorption maximum of the investigated compound (λ_{irr} = 635, 660, or 670 nm). The light intensity was set to 0.300 mW and accurately measured with a radiometer (ILT 1400A/SEL100/F/QNDS2, International Light Technologies). The decay of DPBF absorption at 414 nm (ε^{DPBF} = 2.3 × 10^4 mol^{-1} L cm^{-1}) was detected at 20 °C by a UV–visible spectrophotometer (Varian Cary 50 Scan).

The Φ_Δ values were calculated from Stern–Volmer plots on the basis of eq 1:

$$\frac{1}{\Phi_{DPBF}} = \frac{1}{\Phi_\Delta} + \frac{k_d}{k_r}\frac{1}{\Phi_\Delta}\frac{1}{[DPBF]} \quad (1)$$

where Φ_{DPBF} is the quantum yield of the photoreaction, k_d is the decay rate constant of $^1O_2$ in the solvent and k_r is the rate constant of the reaction of DPBF with $^1O_2$. The $1/\Phi_\Delta$ value was obtained as the intercept of each linear plot ($1/\Phi_{DPBF}$ versus $1/[DPBF]$).

Other Physical Measurements. IR spectra were recorded on a Varian 660-IR FT-IR spectrometer in the range 4000–250 cm^{-1} (KBr pellets). UV–visible solution spectra, other than those for spectroelectrochemistry (see above) were recorded with a Varian Cary 5E spectrometer. Thermogravimetric analyses (TGA) were performed on a Stanton Redcroft model STA-781 analyzer under a N_2 atmosphere (0.5 L/min). Elemental analyses for C, H, and N were provided by the "Servizio di Microanalisi" at the Dipartimento di Chimica, Università "La Sapienza" (Rome) on an EA 1110 CHNS-O instrument. The ICP-PLASMA Pd and Pt analyses were performed on a Varian Vista MPX CCD simultaneous ICP-OES.

RESULTS AND DISCUSSION

Preparative Aspects and IR Spectra. Each $[(PtCl_2)_4LM]$ derivative (M = $Mg^{II}(H_2O)$, Zn^{II}, Pd^{II}, Cu^{II}, and Co^{II}) was synthesized from the respective mononuclear [LM] complex by reaction with $PtCl_2$ under reaction conditions similar to those

dx.doi.org/10.1021/ic301989a | Inorg. Chem. 2012, 51, 12548–12559

Table 1. UV-Visible Spectral Data for $[(PtCl_2)_4LM]$, $[(PdCl_2)_4LM]$ and [LM] in DMSO

	λ (nm) (log ε)					
compound	Soret region		Q-band region			ref.[d]
$[(PtCl_2)_4LMg(H_2O)]$	385 (4.71)		600 (4.22)	628sh (4.26)	659 (5.00)	tw
$[(PdCl_2)_4LMg(H_2O)]$[a]	342	368sh	597		656	tw
$[LMg(H_2O)]$	374 (5.08)	566sh (3.96)	594 (4.36)	629sh (4.55)	653 (5.34)	21
$[(PtCl_2)_4LZn]$	382 (4.91)		603 (4.44)		667 (5.30)	tw
$[(PdCl_2)_4LZn]$	370 (5.03)		598 (4.47)		657 (5.23)	tw
[LZn]	372 (5.10)	565sh(4.02)	592 (4.54)	629sh (4.61)	655 (5.36)	21
$[(PtCl_2)_4LPd]$	345 (5.00)		5.80 (4.44)		639 (5.10)	tw
$[(PdCl_2)_4LPd]$	341 (5.02)	370sh (4.69)	575 (4.34)		636 (5.03)	11
[LPd]	340 (4.94)	380sh (4.68)	575 (4.32)		633 (4.95)	11
$[(PtCl_2)_4LPt]$[b]	323 (4.99)	361 (5.00)	568 (4.48)		627 (5.18)	14
[LPt][b,c]	358		565		626	14
$[(PtCl_2)_4LCu]$[c]	365		600		656	tw
$[(PdCl_2)_4LCu]$	358 (4.79)		593 (4.33)		651 (4.95)	tw
[LCu]	365 (4.91)		590 (4.44)		648 (5.18)	21
$[(PtCl_2)_4LCo]$[c]	367	442	586		640	tw
$[(PdCl_2)_4LCo]$	357 (5.00)	448 (4.43)	587 (4.47)		638 (5.03)	tw
[LCo]	355 (5.23)	450 (4.65)	586sh (4.71)		634 (5.24)	21

[a]The presence of traces of $[(PdCl_2)_4Pd]$ formed during the synthetic procedure (transmetalation) excluded precise definition of ε values. [b]Solution preacidified with HCl ($c = 2.0 \times 10^{-4}$ M) to prevent a one-electron reduction. [c]Spectra of highly aggregated species. [d]tw = this work.

used to obtain the corresponding externally palladated analogues (DMSO, 120 °C, molar ratio macrocycle/$PtCl_2$ 1/8),[11,17] but completion of the reaction to obtain the platinated species required longer reaction times than for the $PdCl_2$ complexes (22 h instead of 5 h). Noteworthy, synthesis of homopentametallic $[(PtCl_2)_4LPt]$ from free-base $[LH_2]$ and $PtCl_2$ (excess) in DMSO at 120 °C takes 5 days to go to completion.[14] Satisfactory elemental analyses were generally obtained for all types of atoms, although the experimental values for nitrogen were often a little lower than the calculated values. This is in line with previous findings for both the $[(PdCl_2)_4LM]$ analogues[17] and a series of heterobimetallic compounds,[13] and it was suggested that the heavy metal centers (Pd, Pt) retain nitrogen during thermal degradation.

The air-stable dark-green amorphous $[(PtCl_2)_4LM]$ materials normally incorporate clathrated water, the amount of which is variable from batch to batch for each compound, as previously reported for related macrocycles.[11,13,14,17] The clathrated water could be easily eliminated by heating under vacuum at mild temperatures (~ 100 °C), but returned upon exposure to the atmosphere. Since water does not significantly influence the spectral or redox behavior of the investigated compounds, the examined species will be formulated hereafter in this paper without showing external water molecules.

Similar IR spectral patterns are observed for the $[(PtCl_2)_4LM]$ complexes, independent of the central metal ion. A common feature in the IR spectra of these compounds is the presence of a medium intensity absorption at about 350 cm^{-1} which is assigned as the $\nu_{(Pt-Cl)}$ mode. This band appears as a double-peaked absorption (344/336 cm^{-1}) in the case of $[(PtCl_2)_4LCo]$, similar to what was reported for $[(PtCl_2)_4LPt]$ (345/334 cm^{-1}).[14] Formation of the externally tetraplatinated species in the conversion of [LM] to $[(PtCl_2)_4LM]$ results in disappearance of the absorptions at 992−994 cm^{-1} and 790 cm^{-1} present for the [LM] species, whereas new absorptions grow in at 770−780 cm^{-1}. An absorption in the range of 955−971 cm^{-1}, also observed for the [LM] species (the exact position depending on the specific central ion of the macrocycle), is still present in the pentanuclear $[(PtCl_2)_4LM]$ species. These IR spectral features are particularly informative for establishing complete formation of the pentanuclear species at the end of the synthetic procedure.

UV−visible Spectral Behavior. The $[(PtCl_2)_4LM]$ and $[(PdCl_2)_4LM]$ complexes are insoluble in both water and organic nondonor solvents (CH_2Cl_2, $CHCl_3$, acetone) and moderately soluble in the low-donor solvents DMSO, pyridine, and DMF ($c = 10^{-4}$ M or a little higher). In these solvents, some of the compounds show aggregation and also a tendency to undergo a one-electron reduction as described below and also reported earlier in the literature for the $[(PdCl_2)_4LM]$ macrocycles.[12,17] As to these latter series of macrocycles, it should be pointed out that previously reported UV−visible spectral data of those with M = $Mg^{II}(H_2O)$, Zn^{II}, and Cu^{II} were measured via spectroelectrochemical experiments using concentrations close to saturation (ca. 10^{-4} M or higher) and in the presence of 0.2 M TBAP.[17] The UV−visible data listed in Tables 1, 2 and Supporting Information, Table S1 in the absence of supporting electrolyte were obtained at lower compound concentrations of about 10^{-5} M (spectroscopic data on the Co^{II} complex $[(PdCl_2)_4LCo]$ are also included in these tables).

DMSO and Pyridine. Tables 1 and Supporting Information, Table S1 summarize the spectral data, either quantitative or qualitative as appropriate, measured for dilute solutions ($c \leq 10^{-5}$ M) of $[(PtCl_2)_4LM]$ and $[(PdCl_2)_4LM]$ (M = $Mg^{II}(H_2O)$, Zn^{II}, Pd^{II}, Pt^{II}, Cu^{II}, Co^{II}) in DMSO and pyridine, respectively. UV−visible spectral data of the corresponding mononuclear

dx.doi.org/10.1021/ic301989a | Inorg. Chem. 2012, 51, 12548−12559

Table 2. UV-Visible Spectral Data of $[(PtCl_2)_4LM]$, $[(PdCl_2)_4LM]$ and [LM] in DMF and DMF/HCl

		λ (nm) (log ε)					
solvent	compound	Soret region		Q-band region			ref.[c]
DMF	$[(PtCl_2)_4LMg(H_2O)]$	383 (4.69)		603 (4.18)		664 (4.96)	tw
	$[(PdCl_2)_4LMg(H_2O)]$[a]	342		600		662	tw
	$[LMg(H_2O)]$	370 (4.94)		597 (4.39)	628sh (4.43)	658 (5.20)	tw
	$[(PdCl_2)_4LZn]$	377 (4.86)	420sh (4.57)	600 (4.38)		662 (5.26)	tw
	[LZn]	375 (4.90)		600 (4.38)	626sh (4.84)	657 (5.15)	tw
DMF/HCl	$[(PtCl_2)_4LMg(H_2O]$	368 (4.72)		600 (4.25)	626sh (4.38)	663 (4.97)	tw
	$[(PdCl_2)_4LMg(H_2O)]$[a]	344		600		664	tw
	$[LMg(H_2O)]$	372 (4.74)		597 (4.20)		654 (4.94)	tw
	$[(PtCl_2)_4LZn]$	395 (4.90)		600 (4.44)	631sh (4.45)	662 (5.34)	tw
	$[(PdCl_2)_4LZn]$	377 (4.86)	423sh (4.57)	600 (4.40)	633sh (4.43)	662 (5.28)	tw
	[LZn]	376 (4.98)		596 (4.45)	626sh (4.50)	657 (5.27)	tw
	$[(PtCl_2)_4LPd]$	347 (4.95)		576 (4.47)		636 (5.18)	tw
	$[(PdCl_2)_4LPd]$	343 (5.00)		575 (4.37)		635 (5.11)	tw
	[LPd]	340 (4.65)	400sh	572 (4.10)		631 (4.68)	tw
	$[(PtCl_2)_4LPt]$	321 (5.08)	364 (4.99)	566 (4.52)		624 (5.26)	14
	[LPt][b]	356		565		621	14
	$[(PtCl_2)_4LCu]$	367 (4.80)		595 (4.38)		655 (5.09)	tw
	$[(PdCl_2)_4LCu]$	370 (4.84)		598 (4.37)		654 (5.05)	tw
	[LCu][b]	370		595		650	tw
	$[(PtCl_2)_4LCo]$	367 (4.90)	440 (4.42)	590 (4.37)		642 (5.00)	tw
	$[(PdCl_2)_4LCo]$	353 (5.00)	429	587 (4.43)		646 (5.25)	tw
	[LCo][b]	353	442	579		634	tw

[a]The presence in the compound of traces of $[(PdCl_2)_4LPd]$ formed during the reaction $[LMg(H_2O)] + PdCl_2$ (transmetalation reaction) prevented a precise calculation of the ε values. [b]Spectra reduced in intensity because of persistent aggregation. [c]tw = this work.

[LM] species, taken under the same solution conditions, are also reported for comparison.

All but one of the $[(PtCl_2)_4LM]$ compounds are stable in their neutral form after being dissolved in DMSO or pyridine. $[(PtCl_2)_4LPt]$ is the exception in that the neutral porphyrazine is gradually reduced to its monoanionic form,[14] thus evidencing the crucial role of the metal center (Pt^{II}) and the four external $PtCl_2$ groups in the facile redox process of the complex (see also following electrochemistry sections). Reducibility for $[(PtCl_2)_4LPt]$ can be prevented in the two solvents by adding HCl (2×10^{-4} M) before dissolution of the compound.[14]

The $[(PtCl_2)_4LMg(H_2O)]$ and $[(PtCl_2)_4LZn]$ complexes show spectra typical of monomers in DMSO and pyridine with absorptions in the Soret region (300−450 nm) and sharp narrow Q bands in the region of 600−700 nm, attributable to ligand-centered $\pi-\pi^*$ transitions. A parallel behavior is seen for the Pd^{II} complex $[(PtCl_2)_4LPd]$ in DMSO, but this compound shows persistent aggregation in pyridine at all concentrations, even as low as $10^{-5}-10^{-7}$ M. Aggregation is also extensive for the analogues with Cu^{II} and Co^{II} central metal ions, and only peak absorption maxima, without molar absorptivities, could be precisely identified in DMSO and pyridine for these compounds in their monomeric form. These values of λ_{max} are given in Tables 1 and Supporting Information, Table S1.

At the concentrations of about 10^{-5} M, all the $[(PdCl_2)_4LM]$ compounds with M = $Mg^{II}(H_2O)$, Zn^{II}, Cu^{II} or Co^{II} exhibit in DMSO absorptions typical of monomeric species (narrow intense Q band). No spectral data are available for $[(PdCl_2)_4LM]$ in pyridine (see Supporting Information, Table S1) because the external $PdCl_2$ units are immediately lost after dissolution in this solvent, leading to formation of the corresponding [LM] species.[12,17] This behavior contrasts with what is observed for the $[(PtCl_2)_4LM]$ complexes which have a high stability in pyridine and retain the external $PtCl_2$ groups for several days or longer, after which the UV−visible spectra indicate some formation of [LM] in solution. Noteworthy, a complete elimination of the exocyclic $PtCl_2$ units from $[(PtCl_2)_4LPt]$ in pyridine requires heating for 3 h at 120 °C.[14]

DMF. Table 2 summarizes the UV−visible data of the $[(PtCl_2)_4LM]$ compounds ($c \leq 10^{-5}$ M) in DMF and DMF containing HCl (2×10^{-4} M). Some of the compounds are aggregated in DMF, and there is also a tendency to undergo a one-electron reduction generating the −1 charged species, a problem encountered in previous studies of related $[(PdCl_2)_4LM]$ compounds.[12,17] This type of reduction in DMF results from an unknown reducing agent (probably dimethylamine) present in the solvent at low concentrations (ca. 10^{-5} M). As to the Mg^{II} and Zn^{II} complexes, the compound $[(PtCl_2)_4LMg(H_2O)]$, minimally contaminated by the presence of the parent species $[(PtCl_2)_4LPt]$, is monomeric in DMF and the hardest to reduce of the examined porphyrazines (see later section) with almost no tendency toward reduction to its monoanion. In constrast, the Zn^{II} analogue, $[(PtCl_2)_4LZn]$, shows peaks due to both the neutral

dx.doi.org/10.1021/ic301989a | Inorg. Chem. 2012, 51, 12548−12559

porphyrazine and the corresponding π-anion radical, $[(PtCl_2)_4LZn]^-$, immediately after dissolution (Figure 2A-a).

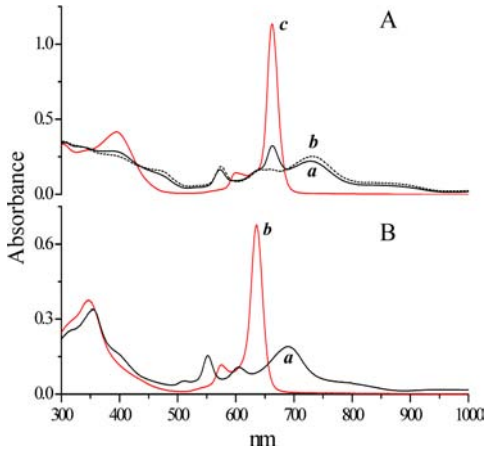

Figure 2. (A) UV−visible spectra of $[(PtCl_2)_4LZn]$ (a) in DMF showing peaks of the reduced species $[(PtCl_2)_4LZn]^-$ at 470, 575, 730 nm, (b) in DMF + $NaBH_4$, (c) in DMF + HCl; (B) (a) $[(PtCl_2)_4LPd]$ in DMF showing peaks of the reduced species $[(PtCl_2)_4LPd]^-$ at 400, 510, 551, 605, 690 nm, (b) in DMF + HCl.

This monoanion can be fully generated by adding a small amount of an appropriate reducing agent to solution ($NaBH_4$; Figure 2A-b) or by controlled potential electroreduction as shown on the following pages.

The complexes $[(PtCl_2)_4LM]$ with M = Pd^{II}, Cu^{II}, and Co^{II} undergo an immediate and complete one-electron reduction in DMF (see spectrum of the Pd^{II} monoanion in Figure 2B-a). Assignment of the spectrum to the −1 charged species is unequivocal, as the number, position, and relative intensities of the absorption peaks approach what was earlier reported for the $[(PtCl_2)_4LPt]$ analogue, which is converted immediately to $[(PtCl_2)_4LPt]^-$ in DMF upon dissolution of the neutral species.[14] Reoxidation of the homogeneously generated monoanions to the corresponding neutral species could be accomplished in DMF upon adding a slight excess of HCl (c = 2×10^{-4} M) to solution. This is illustrated in Figure 2 for the Zn^{II} and Pd^{II} species (Figure 2A-c and 2B-b, respectively). Noteworthy, dissolution of the compounds $[(PtCl_2)_4LM]$ with M = Pd^{II}, Cu^{II}, Co^{II} in preacidified DMF ([HCl]: 2×10^{-4} M) prevents reduction in all cases, and well-defined spectra for monomeric $[(PtCl_2)_4LM]$ are obtained; this is similar to what was observed for $[(PtCl_2)_4LPt]$.[14]

Similarly to the behavior observed in DMSO (see above), the complexes carrying exocyclic $PdCl_2$ units, that is, $[(PdCl_2)_4LM]$ with M = $Mg^{II}(H_2O)$ and Zn^{II}, exhibit UV−visible spectra in DMF and DMF/HCl solutions (c = 10^{-5} M or lower) typical of monomeric species (narrow intense Q band). In contrast to this, the Pd^{II}, Cu^{II} and Co^{II} analogues undergo a one-electron reduction in DMF which can be reversed by addition of 1.0×10^{-4} M HCl. The UV−visible spectra of the $[(PdCl_2)_4LM]$ species were all stable in preacidified DMF (DMF/HCl) with no traces of aggregation or reduction.

A final remark is needed with respect to the spectra of the monometallic [LM] complexes, here reported in DMF and DMF/HCl for the first time. At low concentrations (ca. 10^{-5} M or lower), the Zn^{II} and $Mg^{II}(H_2O)$ derivatives show an initial aggregation which vanishes with time; the final spectra are then stable and indicative of monomeric species. This behavior parallels what was reported in DMSO and pyridine.[18,21] The [LM] species with M = Cu^{II} or Co^{II} undergo partial reduction in DMF. Reduction is inhibited in preacidified DMF (DMF/HCl), but persistent aggregation occurs under these solution conditions. Thus, for these two complexes only qualitative data attributable to the monomeric form of the macrocycle are reported (Table 2).

Several additional observations can be made regarding the spectral data in Tables 1, 2, and Supporting Information, Table S1. The first is that for each individual species there is no significant solvent effect on the position of the Soret (340−390 nm) or the Q bands (630−670 nm). There is, however, an effect of the central metal ion; the Q-band peak is located in the range 620−630 nm for complexes with central Pt^{II}, 630−640 nm for the related Pd^{II} and Co^{II} species, 650−660 nm for the Cu^{II} complex, and 655−670 nm for the complexes with central Mg^{II} or Zn^{II}. Most importantly, the peak position of the Q band moves bathochromically in an extremely reproducible fashion along the sequence [LM] → $[(PdCl_2)_4LM]$ → $[(PtCl_2)_4LM]$ for each single M, thus indicating a progressive decrease in energy of the lowest energy HOMO−LUMO transition consequent to external coordination by the $PdCl_2$ or $PtCl_2$ units. The electronic influence of these units on the π-conjugated central macrocyclic framework is remarkable when considering that not only they are bound at the extreme periphery of the macrocycle but that the exocyclic coordination sites, $N_{2(py)}PdCl_2$ and $N_{2(py)}PtCl_2$, are oriented practically perpendicular to the plane of the central tetrapyrazinoporphyrazine macrocycle (see X-ray structural information on the metalated precursors $[(CN)_2Py_2PyzMCl_2]$ (M = Pd^{II}, Pt^{II}).[11,22] The electrochemical data reported below also indicate a strong influence of the $PdCl_2$ and $PtCl_2$ units on the electronic properties of the molecules.

Electrochemistry and Spectroelectrochemistry. Cyclic voltammetry and thin-layer spectroelectrochemistry of $[(PtCl_2)_4LM]$ (M = Zn^{II}, $Mg^{II}(H_2O)$, Pd^{II}, Cu^{II}, Pt^{II}) were carried out in the same nonaqueous solvents used for the UV−visible spectral studies of the neutral compounds. At the concentrations required for the electrochemical experiments (ca. 10^{-4} M or higher), the Zn^{II}, $Mg^{II}(H_2O)$, and Pd^{II} complexes are all soluble and show no evidence of aggregation. In contrast, the Cu^{II} and Pt^{II} complexes of $[(PtCl_2)_4LM]$ are highly aggregated in their neutral form and required an initial electrochemical solubilization prior to making the measurements. For these two porphyrazines, it was necessary to first scan to negative potentials to generate the more soluble trianion of each compound and then reverse the potential to measure the half wave potentials and UV−visible spectra of each electroreduced species in its monomeric form as was earlier described in the literature.[23] However, in the case of $[(PtCl_2)_4LCo]$, no meaningful electrochemical data could be obtained, even after the initial electrochemical pretreatment.

Examples of thin-layer cyclic voltammograms for $[(PtCl_2)_4LPt]$ and [LPt] in DMSO, 0.2 M TBAP are illustrated in Figure 3. As indicated above, the two compounds are highly aggregated under the electrochemical solution conditions but four well-separated and reversible one-electron reductions are obtained for both porphyrazines on the second potential scan after solubilization as described in the literature.[23]

The first two reductions of $[(PtCl_2)_4LPt]$ in solutions of DMSO give the porphyrazine π-anion radical and dianion and are located at $E_{1/2}$ = −0.03 and −0.42 V in the thin layer cell containing 0.2 M TBAP (see Figure 3). Similar reduction

dx.doi.org/10.1021/ic301989a | Inorg. Chem. 2012, 51, 12548−12559

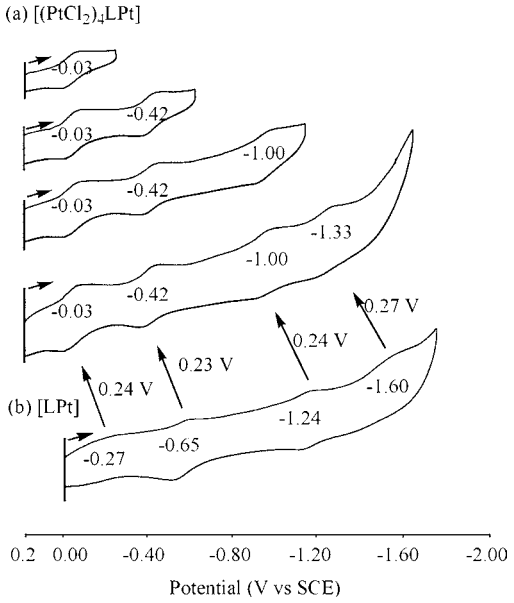

Figure 3. Thin-layer cyclic voltammograms of $[(PtCl_2)_4LPt]$ and [LPt] in DMSO, 0.2 M TBAP on the second potential scan after solubilization via an initial sweep from 0.00 to −1.80 V, as described in the literature.[23]

potentials of −0.03 and −0.39 V are obtained by "regular" cyclic voltammetry (0.1 M TBAP). The first two reductions of [LPt] occur at $E_{1/2}$ = −0.27 and −0.65 V in DMSO, 0.2 M TBAP (Figure 3), and these values are similar to the measured $E_{1/2}$ = −0.25 and −0.61 V for formation of the [LPt] π-anion radical and dianion in DMSO, 0.1 M TBAP (see Table 3). The potential separation between the first and second reductions of $[(PtCl_2)_4LPt]$ and [LPt] are virtually identical for the two compounds in DMSO, and the same is true for the third and fourth reductions, where the two processes are separated by 330 and 360 mV, respectively. In summary, the electrochemical data in Figure 3 indicate a similar overall redox behavior of $[(PtCl_2)_4LPt]$ and [LPt] in DMSO, the only difference between the two compounds being an average positive 245 mV shift of potential for all four one-electron additions to the $PtCl_2$ compound, independent of the overall charge of the molecule.

Similar electrochemical results are obtained for all of the $[(PtCl_2)_4LM]$ and $[(PdCl_2)_4LM]$ complexes with electroinactive M^{II} metal ions, that is, Pd^{II}, Cu^{II}, Zn^{II}, and Mg^{II}. In each case, the binding of $PtCl_2$ or $PdCl_2$ to the molecule leads to a positive potential shift as compared to $E_{1/2}$ values for reduction of [LM] containing the same central metal ion. For example, in DMSO containing 0.1 M TBAP, the easiest to reduce $[(PtCl_2)_4LM]$ species contains a Pd^{II} central metal ion and shows three well-defined reductions ($E_{1/2}$ = 0.00, −0.35, and −0.97 V) while the hardest to reduce $[(PtCl_2)_4LM]$ derivative contains $Mg^{II}(H_2O)$ and exhibits four one-electron reductions at $E_{1/2}$ values of −0.15, −0.49, −1.12, and −1.33 V by routine cyclic voltammetry (CV) at a scan rate of 0.1 V/s. These potentials are summarized in Table 3 along with measured values for each $[(PtCl_2)_4LM]$ and $[(PdCl_2)_4LM]$ complex in DMSO, DMF, and pyridine. Potentials are also listed in Table 3 for [LM] under the same solution conditions.

As seen in Table 3, potentials for the first one-electron reduction of $[(PtCl_2)_4LM]$ show little variation with change of solvent but there is a clear effect of the central metal on the $E_{1/2}$ values as shown for the first reduction in DMSO, 0.1 M TBAP, which follows the order: $Mg^{II}(H_2O)$ (−0.15) → Zn^{II} (−0.10) → Cu^{II} (−0.04) → Pt^{II} (−0.03) → Pd^{II} (0.00). A similar order is maintained for second reduction of the compounds, and this is graphically shown in Figure 4 by the thin-layer cyclic voltammograms measured in DMSO, 0.2 M TBAP.

The combined effect of solvent, central metal ion and compound oxidation state is summarized in Figures 5 and Supporting Information, Figure S1 for the newly investigated compounds. As indicated in Figure 3, the four redox reactions of [LPt] in DMSO containing 0.2 M TBAP are all shifted by a similar amount toward easier reductions upon external coordination of $PtCl_2$ and this is reflected in Figure 5a by the linear plot of $E_{1/2}$ for each reduction of [LPt] vs $E_{1/2}$ for the corresponding reduction of $[(PtCl_2)_4LPt]$. The slope of the plot is 0.98, and the correlation coefficient is 0.9996. A linear relationship is also obtained between $E_{1/2}$ for each reduction of $[LMg(H_2O)]$ and the corresponding reduction of $[(PtCl_2)_4LMg(H_2O)]$ (Supporting Information, Figure S1), but here the slope of the line is 0.89, consistent with a larger influence of $PtCl_2$ on the higher reduced forms of the compounds.

The potential separation between the first reduction of the five $[(PtCl_2)_4LM]$ compounds in DMSO and that of [LM] in the same solvent is shown graphically in Figure 5b. The value averages 200 mV for the first reduction in DMSO while a slightly larger average separation of 214 mV is obtained for the second reduction. The same trend is seen in pyridine and DMF (Supporting Information, Figure S2, a and b, respectively) where $\Delta E_{1/2}$ between the second reductions of [LM] and $[(PtCl_2)_4LM]$ average 224 and 242 mV, respectively. Again, larger separations are seen as the charge on the electroreduced species is increased to −3 and −4 in the last two redox processes.

Almost identical electrochemical behavior is observed in DMSO, DMF, and pyridine for $[(PtCl_2)_4LM]$ and $[(PdCl_2)_4LM]$, although in the latter series of compounds, only the first two reductions have any meaning since the last two process involve [LM] after reduction and loss of the bound $PdCl_2$ groups. Comparisons in pyridine also cannot be made because in this solvent loss of $PdCl_2$ units from $[(PdCl_2)_4LM]$ is immediate with formation of [LM] species, as discussed above and observed elsewhere.[11,17]

In summary, the four reductions of $[(PtCl_2)_4LM]$ in DMSO, DMF, or pyridine are systematically easier than the four reductions of [LM] with the same central metal ion. Similar shifts of potential are observed between $[(PdCl_2)_4LM]$ and [LM] in DMSO and DMF (see Table 3) which demonstrates that external coordination of the $PtCl_2$ or $PdCl_2$ units induces in all cases an easier acceptance of excess negative charge within the macrocyclic framework.

The spectroelectrochemical behavior was examined under experimental conditions slightly different (presence of 0.2 M TBAP, higher concentration of the compounds, $\geq 10^{-4}$ M) from those described above and leading to the UV−visible spectral data listed in Tables 1, 2, and Supporting Information, Table S1. Substantially coincident results are obtained as to both the quantitative data and observed spectral changes, and subtle differences are not taken into account in the following discussion.

The UV−visible spectra for the anions of selected compounds were investigated by thin-layer spectroelectrochemistry. Examples for the UV−visible spectral changes in DMSO

Table 3. Half-Wave Potential Values ($E_{1/2}$, V vs SCE) of the Complexes $[(PtCl_2)_4LM]$ (M = $Mg^{II}(H_2O)$, Zn^{II}, Cu^{II}, Pd^{II}, Pt^{II}, Co^{II}) and Related Species in DMSO, pyridine, and DMF (0.1 M TBAP)

		macrocycle								
solvent	compound	first	second	third	fourth	$PtCl_2$*		Δ_1[b]	Δ_2[c]	ref.[d]
DMSO	$PtCl_2$					−1.20	−1.58			22
	$[(PtCl_2)_4LMg(H_2O)]$	−0.15	−0.49	−1.12	−1.33		−1.78	0.18	0.21	tw
	$[(PtCl_2)_4LZn]$	−0.10	−0.45	−1.10[e]		−1.36	−1.74	0.16	0.22	tw
	$[(PtCl_2)_4LCu]$	−0.04	−0.41	−0.97	−1.25		−1.65	0.18	0.17	tw
	$[(PtCl_2)_4LPt]$	−0.03	−0.39	−0.95		−1.31	−1.78	0.22	0.22	tw
	$[(PtCl_2)_4LPd]$	0.00	−0.35	−0.97		−1.30	−1.78	0.26	0.25	tw
	$PdCl_2$						−0.86			17
	$[(PdCl_2)_4LMg(H_2O]$[a]	−0.15					−1.00	0.18		17
	$[(PdCl_2)_4LZn]$	−0.13	−0.54	−1.39	−1.63		−1.03	0.13	0.13	17
	$[(PdCl_2)_4LCu]$	−0.03	−0.41	−1.24	−1.60		−0.93	0.19	0.17	17
	$[(PdCl_2)_4LPd]$	0.00	−0.37	−1.24	−1.59		−0.85	0.26	0.23	11
	$[LMg(H_2O)]$	−0.33	−0.70	−1.39	−1.67					21
	[LZn]	−0.26	−0.67	−1.38	−1.64					21
	[LCu]	−0.22	−0.58	−1.22	−1.58					21
	[LPd]	−0.26	−0.60	−1.26	−1.61					11
	[LPt]	−0.25	−0.61							tw
	[LCo]	−0.06	−0.76	−1.31	−1.77					21
DMF	$PtCl_2$						−1.79			22
	$[(PtCl_2)_4$ $LMg(H_2O]$	−0.17	−0.52	−1.11	−1.34		−1.78	0.25	0.28	tw
	$[(PtCl_2)_4LZn]$	−0.15	−0.50	−1.07[e]			−1.76	0.24	0.25	tw
	$[(PtCl_2)_4LCu]$	−0.03	−0.41	−1.00	−1.23		−1.76	0.23	0.20	tw
	$[(PtCl_2)_4LPt]$	−0.02	−0.41	−0.95	−1.30		−1.72	0.18	0.22	tw
	$[(PtCl_2)_4LPd]$	0.03	−0.36	−0.97			−1.76	0.22	0.26	tw
	$PdCl_2$						−0.86			17
	$[(PdCl_2)_4LMg(H_2O]$	−0.15	*a*	*a*	*a*		−1.06	0.27		17
	$[(PdCl_2)_4LZn]$	−0.12	−0.52	−1.39	−1.62		−1.00	0.27	0.23	17
	$[(PdCl_2)_4LCu]$	0.00	−0.43	−1.27	−1.62		−1.02			17
	$[(PdCl_2)_4LPd]$	0.04	−0.37	−1.27	−1.62		−1.03	0.29	0.25	17
	$[LMg(H_2O)]$	−0.42	−0.80	−1.43						tw
	[LZn]	−0.39	−0.75	−1.41						tw
	[LCu]	−0.26	−0.61	1.29	−1.61					tw
	[LPt]	−0.20	−0.63	−1.22						tw
	[LPd]	−0.25	−0.62	−1.29	−1.61					tw
	[LCo]	−0.02	−0.84	−1.41	−1.78					tw
py	$PtCl_2$					−1.54	−1.75			22
	$[(PtCl_2)_4LMg(H_2O]$	−0.20	−0.55	−1.14	−1.37		−1.74	0.20	0.24	tw
	$[(PtCl_2)_4LZn]$	−0.18	−0.52	−1.05[e]			−1.77	0.16	0.20	tw
	$[(PtCl_2)_4LCu]$	−0.06	−0.42	−1.01	−1.30		−1.75	0.24	0.26	tw
	$[(PtCl_2)_4LPt]$	−0.05	−0.46	−0.98		−1.46	−1.72			tw
	$[(PtCl_2)_4LPd]$	−0.02	−0.47	−1.01		−1.46	−1.76	0.24	0.19	tw
	$[LMg(H_2O]$	−0.40	−0.79	−1.43	−1.70					21
	[LZn]	−0.34	−0.72	−1.38	−1.66					21
	[LCu]	−0.30	−0.68	−1.28	−1.61					21
	[LPd]	−0.26	−0.66	−1.29	−1.64					11
	[LPt]									tw
	[LCo]	−0.26	−0.87	−1.37	−1.83					21

[a]Badly resolved peaks because of the presence of the transmetalation contaminant $[(PdCl_2)_4LPd]$. [b]Δ_1 = difference in $E_{1/2}$ between first reduction of [LM] and $[(PtCl_2)_4LM]$ or $[(PdCl_2)_4LM]$. [c]Δ_2 = difference in $E_{1/2}$ between second reduction of [LM] and $[(PtCl_2)_4LM]$ or $[(PdCl_2)_4LM]$. [d]This work. [e]Irreversible peak. Value is E_p at scan rate 0.1 V/s.

during the first two one-electron reductions are shown in Figure 6 for $[(PtCl_2)_4LZn]$ and in Supporting Information, Figure S3 for $[(PtCl_2)_4LMg(H_2O)]$, and $[(PtCl_2)_4LPt]$. The isosbestic points in the spectra indicate the lack of detectable intermediates upon going from the neutral form of the complexes to the corresponding −1 and −2 charged species. For all three compounds, the first reduction leads to a decrease in the Q-band intensity and the appearance of typical low intensity absorption bands at 540−570 nm as the anion radicals of $[(PtCl_2)_4LM]$ are generated. The same changes were observed in pyridine and DMF and these changes differ little with change in central metal ion or external coordination (Pd^{II},

dx.doi.org/10.1021/ic301989a | Inorg. Chem. 2012, 51, 12548−12559

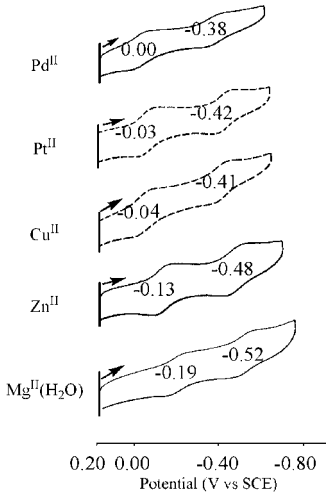

Figure 4. Thin-layer cyclic voltammograms with added $E_{1/2}$ values (V vs SCE) of $[(PtCl_2)_4LM]$ (M = Pd^{II}, Pt^{II}, Cu^{II}, Zn^{II}, $Mg^{II}(H_2O)$) in DMSO containing 0.2 M TBAP. Scan rate = 20 mV/s. Data for $Mg^{II}(H_2O)$, Zn^{II} and Pd^{II} compounds was obtained on the first scan (solid line) while the Pt^{II} and Cu^{II} derivatives require presolubilization and show the second scan (dashed line).

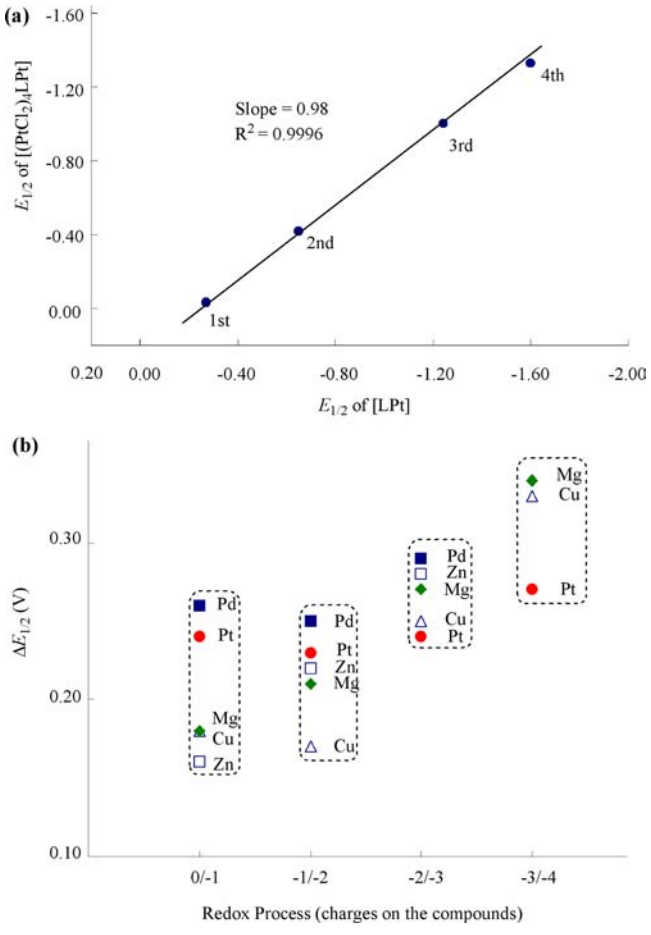

Figure 5. (a) Plot showing linear relationship between $E_{1/2}$ values for each reduction of [LPt] and $[(PtCl_2)_4LPt]$ in DMSO containing 0.1 M TBAP and (b) positive shift of reduction potential ($\Delta E_{1/2}$) for each reduction upon going from [LM] to $[(PtCl_2)_4LM]$ as a function of redox process and central metal ion where M = Pd^{II}, Pt^{II}, Cu^{II}, $Mg^{II}(H_2O)$, or Zn^{II} under the same solution conditions.

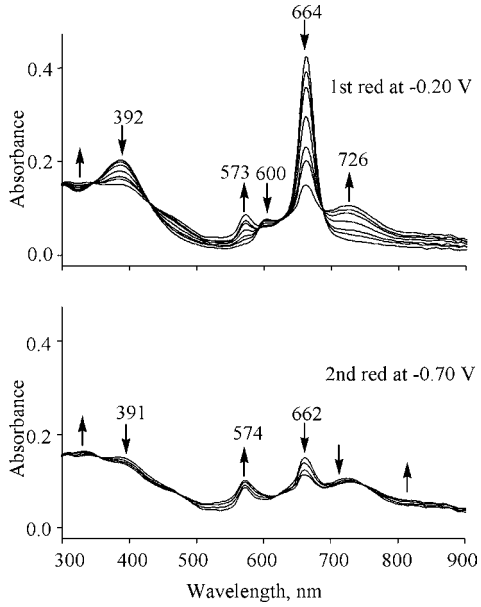

Figure 6. UV−visible spectral changes obtained during the first and second reductions of $[(PtCl_2)_4LZn]$ in DMSO containing 0.2 M TBAP. The cyclic voltammogram of $[(PtCl_2)_4LZn]$ (Figure 4) is characterized by $E_{1/2}$ values of −0.13 and −0.48 V for the first two one-electron reductions.

Pt^{II}). A clear explanation for this resides in the fact that the reductions are exclusively centered on the central porphyrazine core. Similar types of spectral changes upon reductions have been reported for related porphyrazines,[18,21] as exemplified in Supporting Information, Figure S4 in the case of the Pd^{II} complexes. Moreover, such types of spectral changes, indicative of the same sequence of reductions, are observed for porphyrazine analogues in which the central macrocycle is the tetrakis(thiadiazol)porphyrazine dianion TTDPz. Detailed DFT(TDDFT) calculations led to an accurate interpretation of the UV−visible spectra for the neutral species [TTDPzM] (M = Zn^{II}, $Mg^{II}(H_2O)$, Cu^{II}, $2H^{I}$)[24] and for the series of negatively charged $[TTDPzM]^{n-}$ (n = 1−4) using the Zn^{II} complex [TTDPzZn] as a representative example.[23a]

Singlet Oxygen Quantum Yields. As mentioned above, the involvement of porphyrins and related macrocycles (chlorines, bacteriochlorins, phthalocyanines, naphthalocyanines, texapyrines) as photosensitizers for the generation of $^1O_2$ is well-known,[1] but porphyrazines have received in general only limited attention in this regard (see refs 3−5 and our most recent work[12−14,20]).

The efficiency of porphyrazine photosensitizers will depend upon their tendency to undergo, upon light irradiation, an excitation from the ground state S_0 to the triplet state T_1 with high quantum yield, and have a T_1 adequate energy and lifetime to allow for a proper energy transfer to dioxygen for the process $^3O_2 \rightarrow {}^1O_2$ to occur. The type of central metal ion in the macrocycle can strongly influence this process and, in this regard, it is known that closed shell metal ions like Zn^{II} and Mg^{II} can lead to high photoactivity. To our knowledge, our recent studies[11,13,14,20] appear to contain the first reported examples where Pd^{II} or Pt^{II} is incorporated into the central cavity of a porphyrazine macrocycle. Following our most recent results on the homometallic pentanuclear Pt^{II} complex $[(PtCl_2)_4LPt]$, it appeared worthwhile as a main target of the present work to explore the photosensitizing activity of the new

dx.doi.org/10.1021/ic301989a | Inorg. Chem. 2012, 51, 12548−12559

Table 4. Singlet Oxygen Quantum Yields (Φ_Δ) in DMF and/or DMF Preacidified with HCl ($1-2 \times 10^{-4}$ M)

photosensitizer	HCl [M]	λ_{max} [nm]	λ_{irr} [nm]	Φ_Δ[a]	ref.[e]
[LZn]	0	657	660	0.55[b]	13
	1×10^{-4}	657	660	0.58	13
[$(PdCl_2)$LZn]	0	656	660	0.53	13
	1×10^{-4}	656	660	0.58	13
[$(PtCl_2)$LZn]	0	658	660	0.53	13
	1×10^{-4}	658	660	0.57	13
[$(PtCl_2)(CH_3)_6$LZn]$^{6+}$	1×10^{-4}	664	660	0.46	13
[$(PdCl_2)_4$LZn]	0	662	670	0.48	tw
	1×10^{-4}	662	670	0.52	tw
[$(PtCl_2)_4$LZn]	2×10^{-4}	663	660	0.55	tw
[$(CH_3)_8$LZn]$^{8+}$	0	665	660	0.29	tw
	$1-2 \times 10^{-4}$	665	660	0.39	tw
[LMg(H_2O)]	0	658	660	0.09	13
	1×10^{-4}	653	660	0.29	13
[$(PdCl_2)$LMg(H_2O)]	0	657	660	0.06	13
	1×10^{-4}	654	660	0.29	13
[$(PtCl_2)$LMg(H_2O)]	0	660	660	0.08	13
	1×10^{-4}	654	660	0.40	13
[$(PtCl_2)(CH_3)_6$LMg(H_2O)]$^{6+}$	0	669	660	0.08	13
	1×10^{-4}	665	660	0.28	13
[$(PdCl_2)_4$LMg(H_2O)]	0	662	670	0.23	tw
	1×10^{-4}	660	670	0.37	tw
[$(PtCl_2)_4$LMg(H_2O)]	0	667	660	0.17	tw
	2×10^{-4}	660	660	0.56	tw
[$(CH_3)_8$LMg(H_2O)]$^{8+}$	0	669	660	0.02	tw
	2×10^{-4}	664	660	0.26	tw
[LPd]	1×10^{-4}	631	635	0.55[d]	13
[$(PdCl_2)$LPd]	1×10^{-4}	633	635	0.52	13
[$(PtCl_2)$LPd]	1×10^{-4}	631	635	0.43	13
[$(PtCl_2)(CH_3)_6$LPd]$^{6+}$	1×10^{-4}	637	635	0.20	13
[$(PdCl_2)_4$LPd]	1×10^{-4}	635	635	0.56[d]	14
[$(PtCl_2)_4$LPd]	2×10^{-4}	636	635	0.51	tw
[$(CH_3)_8$LPd]$^{8+}$	1×10^{-4}	638	635	0.15[d]	tw
[LPt]	2×10^{-4}	621	635	0.13	14
[$(PtCl_2)_4$LPt]	2×10^{-4}	624	635	0.36	14
[$(CH_3)_8$LPt]$^{8+}$	2×10^{-4}	626	635	0.20	14

[a]Mean value of at least three measurements. Uncertainty is half dispersion and it is typically ±0.03. [b]A Φ_Δ value of 0.53 was measured in pyridine.[27] [d]More reliable Φ_Δ values, lower than those reported previously[12] which were obtained by the comparative method. [e]tw = this work.

heteropentanuclear species [$(PtCl_2)_4$LM] where M = Zn^{II}, Mg^{II} or Pd^{II}.

Table 4 lists the singlet oxygen quantum yields (Φ_Δ) of the pentanuclear species [$(M'Cl_2)_4$LM] (M′ = Pd^{II}, Pt^{II}; M = Zn^{II}, $Mg^{II}(H_2O)$, Pd^{II}, Pt^{II}) measured in DMF and/or DMF preacidified with HCl ($1-2 \times 10^{-4}$ M) by an absolute method (see details in Experimental Section). Data for the related neutral mono-, homo-, and heterobinuclear complexes, as well as the hexa- and octacationic species, the majority of which was previously reported,[13,14] are also included in Table 4 for comparison purposes. As can be seen in the table, Φ_Δ values were obtained in both DMF and preacidified DMF for all the listed complexes carrying centrally Zn^{II} and Mg^{II} except for the Zn^{II} complexes [$(PtCl_2)(CH_3)_6$LZn]$^{6+}$ and [$(PtCl_2)_4$LZn]. For these latter two species and for all the compounds with central Pd^{II} and Pt^{II} data were only obtained in the DMF/HCl mixture, because of the compound's facile reducibility to the corresponding −1 charged species in the absence of HCl. UV−visible data and the Stern−Volmer plot of a typical experiment used to calculate the Φ_Δ values of the sensitizers, according to eq 1 are shown in Figure 7 for [$(PtCl_2)_4$LZn].

As can be seen in Table 4, only small differences of the Φ_Δ values are observed for the Zn^{II} complexes measured in DMF or DMF/HCl. The low effect of acidification seen on the photosensitizing activity in DMF/HCl seems to indicate that the added excess protons only negligibly perturb the central Zn^{II}-macrocyclic framework. There is instead evidence for a larger influence of acidification on the Φ_Δ values of the pentanuclear Mg^{II} species [$(PdCl_2)_4$LMg(H_2O)] and [$(PtCl_2)_4$LMg(H_2O)] and, as already reported elsewhere[13] for the related series of complexes carrying centrally Mg^{II}, the values being in all cases significantly higher in DMF/HCl than in DMF. This problematic aspect might be related to changes of coordination which occur at the axial sites of Mg^{II}, a point which necessitates further inspection.

The high Φ_Δ values found for the Zn^{II} species [$(PdCl_2)_4$LZn] (0.48; 0.52) and [$(PtCl_2)_4$LZn] (0.55) fall in the range of the other Zn^{II} ligand-related neutral species also

dx.doi.org/10.1021/ic301989a | Inorg. Chem. 2012, 51, 12548−12559

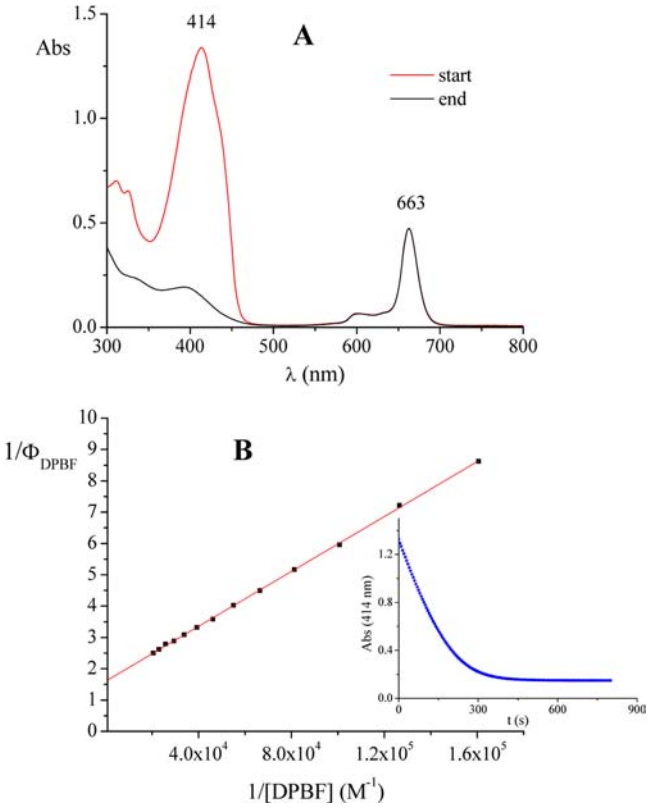

Figure 7. (A) UV–visible spectra of a DMF/HCl solution ([HCl] = 2 × 10^{-4} M) containing $[(PtCl_2)_4LZn]$ and DPBF before (red line) and after (black line) laser irradiation; (B) Stern–Volmer data analysis of the DPBF photooxidation (shown in the inset).

listed in Table 4 (obtained under similar experimental conditions) and identify them as potent photosensitizers. These data are in line with expectation, as the observed Φ_Δ values for a number of Zn^{II} phthalocyanine[2,25] and porphyrazine analogues,[4,26] also obtained in DMF, normally fall in the range 0.4–0.7. The Φ_Δ values shown in Table 4 for the parallel series of Mg^{II} complexes are generally lower (with only one exception) than those of the corresponding Zn^{II} species; these findings are as expected for the "heavy atom effect", which favors Zn^{II}. The Φ_Δ values of the neutral complexes with a central Pd^{II} ion, that is, [LPd], $[(PdCl_2)LPd]$, $[(PtCl_2)LPd]$, $[(PdCl_2)_4LPd]$, and $[(PtCl_2)_4LPd]$, measured exclusively in DMF/HCl, compare well with compounds having a central Zn^{II} ion, thus showing comparable photosensitizing activity (Φ_Δ = 0.5–0.6).

It is interesting to observe that when moving along the series of the neutral mono-, bi-, and pentametallic species with fixed central metal ion, no significant changes of Φ_Δ are observed for the Zn^{II} compounds (Φ_Δ values in parentheses in DMF and/or exclusively in DMF/HCl): [LZn] (0.52; 0.58), $[(PdCl_2)LZn]$ (0.53; 0.58), $[(PtCl_2)LZn]$ (0.53; 0.57); $[(PdCl_2)_4LZn]$ (0.48; 0.52); $[(PtCl_2)_4LZn]$ (0.55). The sequence of the Pd^{II} analogues (data only in DMF/HCl, Table 4) behaves similarly. The Mg^{II} compounds are more sensitively affected by the introduction of $PdCl_2$ and $PtCl_2$ units, as can be seen in the sequence: $[LMg(H_2O)]$ (0.09; 0.29), $[(PdCl_2)LMg(H_2O)]$ (0.06; 0.29), $[(PtCl_2)LMg(H_2O)]$ (0.08; 0.40); $[(PdCl_2)_4LMg(H_2O)]$ (0.23; 0.37); $[(PtCl_2)_4LMg(H_2O)]$ (0.17; 0.56). In addition, the level of progressive increment of the Φ_Δ values is more effective for the $PtCl_2$ units than for $PdCl_2$. It can also be observed that the quaternization process of the pyridine N atoms, with formation of the +6 and +8 charged species, partly affects the efficiency of $^1O_2$ generation, as can be seen in the sequences (Φ_Δ data in parentheses in DMF and DMF/HCl where available): $[(PtCl_2)LZn]$ (0.53; 0.58) → $[(PtCl_2)(CH_3)_6LZn]^{6+}$ (0.46) → $[(CH_3)_8LZn]^{8+}$ (0.29; 0.39); $[(PtCl_2)LMg(H_2O)]$ (0.08; 0.40) → $[(PtCl_2)(CH_3)_6LMg(H_2O)]^{6+}$ (0.08; 0.28) → $[LMg(H_2O)]^{8+}$ (0.02; 0.26); $[(PtCl_2)LPd]$ (0.43) → $[(PtCl_2)(CH_3)_6LPd]^{6+}$ (0.20) → $[(CH_3)_8LPd]^{8+}$ (0.15), with the couple of the Pt^{II} species [LPt] (0.13) → $[(CH_3)_8LPt]^{8+}$ (0.20) representing an exception.

The global set of Φ_Δ values summarized in Table 4 indicates that within the context of all the presently discussed pyrazinoporphyrazines the majority of the species, particularly those with central Zn^{II} and Pd^{II} ions, behave as potent photosensitizers for $^1O_2$ production and can be seen as promising anticancer agents in PDT. In addition, the compounds carrying peripherally cis-platin-like functionalities may open up possibilities of their use as bimodal anticancer curative agents. As to the above-mentioned water-soluble hexacation $[(PtCl_2)(CH_3)_6LZn]^{6+}$, its previously reported PDT/G4 bimodal potentialities,[16] shortly reminded above, and the investigated role of the exocyclic cis-platin-like functionality may add further significance to the multimodal anticancer potentialities of this interesting species. The newly described pentanuclear compounds $[(PtCl_2)_4LM]$ (M = Zn^{II}, $Mg^{II}(H_2O)$, Pd^{II}, Pt^{II}), which behave as active photosensitizers for $^1O_2$ generation, are rare examples of tetrapyrrolic macrocycles characterized by the presence of multiple cis-platin-like functionalities.

CONCLUSIONS

The newly presented heterometallic complexes having the formula $[(PtCl_2)_4LM]$ with M = Zn^{II}, $Mg^{II}(H_2O)$, Pd^{II}, Cu^{II} and Co^{II} were studied in conjunction with the previously reported homometallic analogue $[(PtCl_2)_4LPt]$.[14] The parent mono- and pentanuclear species, [LM] and $[(PdCl_2)_4LM]$ respectively, together with related bimetallic and positively charged macrocycles, were also studied in detail. Aggregation phenomena and reducibility to their corresponding −1 charged species were observed for many of the compounds. The UV–visible spectra and electrochemical data of the pentanuclear species $[(PtCl_2)_4LM]$ and their externally palladated analogues $[(PdCl_2)_4LM]$ unequivocally indicate that exocyclic coordination of $PtCl_2$ and $PdCl_2$ units to the [LM] species sensibly modifies the electronic distribution within the central pyrazinoporphyrazine macrocycle, enhancing the electron-deficiency of the entire macrocyclic framework, the $PtCl_2$ and $PdCl_2$ units producing a distinct effect ($PtCl_2$ > $PdCl_2$).

As a central point of this contribution, it was shown that the species $[(PtCl_2)_4LM]$ with M = Zn^{II}, $Mg^{II}(H_2O)$, Pd^{II} and Pt^{II}, and their analogues $[(PdCl_2)_4LM]$ in DMF and/or preacidified DMF behave in many cases as excellent photosensitizers for $^1O_2$ production, the main citotoxic agent in PDT. Among the different species examined, the externally platinated $[(PtCl_2)_4LM]$, particularly those with M = Zn^{II} or Pd^{II} are of special interest because of the presence of peripheral cis-platin-like functionalities in the compounds which provide potentialities for a bimodal photochemotherapeutic anticancer curative modality, a step forward with respect to the exclusive use in PDT.

dx.doi.org/10.1021/ic301989a | Inorg. Chem. 2012, 51, 12548–12559

■ ASSOCIATED CONTENT

Supporting Information

Further details are given in Table S1 and Figures S1−S4. This material is available free of charge via the Internet at http://pubs.acs.org.

■ AUTHOR INFORMATION

Corresponding Author

*E-mail: mariapia.donzello@uniroma1.it (M.P.D.), kkadish@uh.edu (K.M.K.).

Notes

The authors declare no competing financial interest.

■ ACKNOWLEDGMENTS

Financial support by the University of Rome La Sapienza (Ateneo 2010 and 2011), the Robert A. Welch Foundation (K.M.K. Grant E-680) is gratefully acknowledged. M.P.D. is grateful for scientific contributions by the Consorzio Interuniversitario di Ricerca in Chimica dei Metalli nei Sistemi Biologici (CIRCMSB). Thanks are expressed to Prof. L. Mannina (University of Rome) for helpful discussions. M.P.D. is grateful to Maria Luisa Astolfi for ICP-PLASMA analyses.

■ REFERENCES

(1) (a) Ethirajan, M.; Chen, Y.; Joshi, P.; Pandey, R. K. *Chem. Soc. Rev.* **2011**, *40*, 340−362. (b) Celli, J. P.; Spring, B. Q.; Rizvi, I.; Evans, C. L.; Samkoe, K. S.; Verma, S.; Pogue, B. W.; Hasan, T. *Chem. Rev.* **2010**, *110*, 2795−2838. (c) Moreira, L. M.; Vieira dos Santos, F.; Pereira Lyon, J.; Maftoum-Costa, M.; Pacheco-Soares, C.; Soares da Silva, N. *Aust. J. Chem.* **2008**, *61*, 741−754. (d) O'Connor, A. E.; Gallagher, W. M.; Byrne, A. T. *Photochem. Photobiol.* **2009**, *85*, 1053. (e) Szacilowski, K.; Macyk, W.; Drzewiecka-Matuszek, A.; Brindell, M.; Stochel, G. *Chem. Rev.* **2005**, *105*, 2647−2694.

(2) (a) Shinohara, H.; Tsaryova, O.; Schnurpfeil, G.; Wöhrle, D. *J. Photochem. Photobiol., A* **2006**, *184*, 50. (b) Spiller, W.; Kliesch, H.; Wöhrle., D.; Hackbarth, S.; Röder, B.; Schnurpfeil, G. *J. Porphyrins Phthalocyanines* **1998**, *2*, 145. (c) Schnurpfeil, G.; Sobbi, A. K.; Spiller, W.; Kliesch, H.; Wöhrle., D. *J. Porphyrins Phthalocyanines* **1997**, *1*, 159. (d) Fernandez, D. A.; Awruch, J.; Dicelio, L. E. *Photochem. Photobiol.* **1996**, *63*, 784. (e) Müller, S.; Mantareva, V.; Stoichkova, N.; Kliesch, H.; Sobbi, A.; Wöhrle., D.; Shopova, M. *J. Photochem. Photobiol., B* **1996**, *35*, 167. (f) Maree, S. E.; Nyokong, T. *J. Porphyrins Phthalocyanines* **2001**, *5*, 782. (g) Lawrence, D. S.; Whitten, D. G. *Photochem. Photobiol.* **1996**, *64*, 923.

(3) (a) Zimcik, P.; Novakova, V.; Miletin, M.; Kopecky, K. *Macroheterocycles* **2008**, *1*, 21 , and refs therein. (b) Zimcik, P.; Miletin, M.; Novakova, V.; Kopecky, K.; Nejedla, M.; Stara, V.; Sedlackova, K. *Aust. J. Chem.* **2009**, *62*, 425. (c) Novakova, V.; Morkved, E. H.; Miletin, M.; Zimcik, P. *J. Porphyrins Phthalocyanines* **2010**, *14*, 582. (d) Mitzel, F.; Fitzgerald, S.; Beeby, A.; Faust, R. *Eur. J. Org. Chem.* **2004**, 1136.

(4) (a) Baum, S. M.; Trabanco, A. A.; Montalban, A. G.; Micallef, A. S.; Zhong, C.; Meunier, H. G.; Suhling, K.; Phillips, D.; White, A. J. P.; Williams, D. J.; Barrett, A. G. M.; Hoffman, B. M. *J. Org. Chem.* **2003**, *68*, 1665. (b) Sakellariou, E. G.; Montalban, A. G.; Meunier, Hubert, Rumbles, G.; Philips, D.; Ostier, R. B.; Suhling, K.; Barrett, A. G. M.; Hoffman, B. M. *Inorg. Chem.* **2002**, *41*, 2182. (c) Montalban, A. G.; Baum, S. M.; Barrett, A. G. M.; Hoffman, B. M. *Dalton Trans.* **2003**, 2093.

(5) Michelsen, U.; Kliesch, H.; Schnurpfeil, G.; Sobbi, A. K.; Wöhrle, D. *Photochem. Photobiol.* **1996**, *64*, 694.

(6) Klein, A. V.; Hambley, T. W. *Chem. Rev.* **2009**, *109*, 4911−4920.

(7) (a) Lu, Q.-B. *J. Med. Chem.* **2007**, *50*, 2601. (b) Crescenzi, E.; Chiavello, A.; Canti, G.; Reddi, E.; Veneziani, B. M.; Palombo, G. *Mol. Cancer Ther.* **2006**, *5*, 776. (c) Crescenzi, E.; Varriale, E.; Iovino, M.; Veneziani, B. M.; Palumbo, G. *Mol. Cancer Ther.* **2004**, *3*, 537. (d) Nonaka, M.; Ikeda, H.; Inokuchi, T. *Cancer Lett.* **2002**, *184*, 171.

(8) (a) Lottner, C.; Knuechel, R.; Bernhardt, G.; Brunner, H. *Cancer Lett.* **2004**, *203*, 171. (b) Brunner, H.; Arndt, M. R.; Treittinger, B. *Inorg. Chim. Acta* **2004**, *357*, 1649. (c) Brunner, H.; Shellerer, K. -M. *Inorg. Chim. Acta* **2003**, *350*, 39. (cc) Song, R.; Kim, Y.-S.; Sohn, Y. S. *J. Inorg. Biochem.* **2002**, *83*, 83.

(9) (a) Canti, G.; Nicolin, A.; Cubeddu, R.; Taroni, P.; Bandieramonte, G.; Valentini, G. *Cancer Lett.* **1998**, *125*, 39.

(10) (a) Mao, J.; Zhang, Y.; Zhu, J.; Zhang, C.; Guo, Z. *Chem. Commun.* **2009**, 908. (b) Nemykin, V. N.; Mytsyk, V. M.; Volkov, S. V.; Kobayashi, N. *J. Porphyrins Phthalocyanines* **2000**, *4*, 551.

(11) Donzello, M. P.; Viola, E.; Cai, X.; Mannina, L.; Rizzoli, C.; Ricciardi, G.; Ercolani, C.; Kadish, K. M.; Rosa, A. *Inorg. Chem.* **2008**, *47*, 3903.

(12) Donzello, M. P.; Viola, E.; Bergami, C.; Dini, D.; Ercolani, C.; Giustini, M.; Kadish, K. M.; Meneghetti, M.; Monacelli, F.; Rosa, A.; Ricciardi, G. *Inorg. Chem.* **2008**, *47*, 8757.

(13) Donzello, M. P.; Vittori, D.; Viola, E.; Manet, I.; Mannina, L.; Cellai, L.; Monti, S.; Ercolani, C. *Inorg. Chem.* **2011**, *50*, 7391.

(14) Donzello, M. P.; Viola, E.; Mannina, L.; Barteri, M.; Fu, Z.; Ercolani, C. *J. Porphyrins Phthalocyanines* **2011**, *15*, 984.

(15) Manet, I.; Manoli, F.; Donzello, M. P.; Viola, E.; Andreano, G.; Masi, A.; Cellai, L.; Monti, S. *Org. Biol. Chem.* **2011**, *9*, 684.

(16) Manet, I.; Manoli, F.; Donzello, M. P.; Ercolani, C.; Vittori, D.; Cellai, L.; Masi, A.; Monti, S. *Inorg. Chem.* **2011**, *50*, 7403.

(17) Donzello, M. P.; Viola, E.; Cai, X.; Mannina, L.; Ercolani, C.; Kadish, K. M. *Inorg. Chem.* **2010**, *49*, 2447.

(18) Donzello, M. P.; Ou, Z.; Dini, D.; Meneghetti, M.; Ercolani, C.; Kadish, K. M. *Inorg. Chem.* **2004**, *43*, 8637.

(19) Lin, X. Q.; Kadish, K. M. *Anal. Chem.* **1985**, *57*, 1489.

(20) Donzello, M. P.; Viola, E.; Giustini, M.; Monacelli, F.; Ercolani, C. *Dalton Trans.* **2012**, *41*, 6112.

(21) Bergami, C.; Donzello, M. P.; Monacelli, F.; Ercolani, C.; Kadish, K. M. *Inorg. Chem.* **2005**, *44*, 9862.

(22) Cai, X.; Donzello, M. P.; Viola, E.; Rizzoli, C.; Ercolani, C.; Kadish, K. M. *Inorg. Chem.* **2009**, *48*, 7086.

(23) (a) Donzello, M. P.; Ercolani, C.; Cai, X.; Kadish, K. M.; Ricciardi, G.; Rosa, A. *Inorg. Chem.* **2009**, *48*, 9890. (b) De Mori, G.; Fu, Z.; Viola, E.; Cai, X.; Ercolani, C.; Donzello, M. P.; Kadish, K. M. *Inorg. Chem.* **2011**, *50*, 8225.

(24) Donzello, M. P.; Ercolani, C.; Kadish, K. M.; Ricciardi, G.; Rosa, A.; Stuzhin, P. A. *Inorg. Chem.* **2007**, *46*, 4145.

(25) (a) Ogunsipe, A.; Maree, D.; Nyokong, T. *J. Mol. Struct.* **2003**, *650*, 131.

(26) Musil, Z.; Zimcik, P.; Miletin, M.; Kopecky, K.; Petrik, P.; Lenco, J. *J. Photochem. Phtobiol., A* **2007**, *186*, 316.

(27) Morkved, E. H.; Afseth, N. K.; Zimcik, P. *J. Porphyrins Phthalocyanines* **2007**, *11*, 130.